N86-12770

Thin Film Module
Electrical Configuration vs. Electrical Performance

Don L. Morel
ARCO Solar, Inc.
Chatsworth, California

INTRODUCTION

In spite of the worldwide interest in thin film Si:H (TFS) as the leading thin film PV material, relatively few reports on module and device design have appeared. The differences in performance and design options for TFS relative to crystalline Si are significant enough to warrant redevelopment of much of the current design methodology which is largely based on crystalline Si. In Section I below, several aspects of this design issue which have been addressed by the author will be reviewed. The intent here is merely to highlight the main points of those studies since they relate to the discussion in the following section and to the general issues of TFS module design. In the second section the effect of module stability on design is discussed. The changes in module output as they are presently known and understood impact future designs as well as some of what has already been done where constant output was assumed. Only the drop in initial output is treated below. Daily and seasonal increases in output due to annealing will be treated in future studies.

I. REVIEW OF PERTINENT TFS MODULE DESIGN ISSUES

One of the early attempts at understanding how TFS based modules might work under actual outdoor conditions involved use of a Weather/Insolation simulation model (Ref. 1). The then known properties of early modules were fed into the model which could then predict performance at any location for an actual year in terms of total energy delivery. The results are summarized in Table 1 from that study.

Table 1. Yearly Energy (Watt-Hours) Derived from PVSYS Runs for Cz and Si:H Modules

Location	Cz Si	TF Si:H	Ratio TF/Cz
Chatsworth, California	16945	6794	0.4009
Victorville, California	18256	7319	0.4009
Perth, Australia	16115	6493	0.4029

The model had previously been used for crystalline Si (Cz Si). One of the outcomes of the exercise was a direct comparison with Cz Si. It was shown that on an energy delivery basis, TFS modules enjoyed a ~5% relative advantage over their Cz counterparts if they were identical in peak output. This advantage was partially due to FF intensity dependence caused by transparent conductor sheet resistance properties. Ongoing studies along these lines indicate continual modifications in performance which require renewed assessments. In general, TFS module design can be tuned to take full advantage of such differential behavior. The addition of stability performance to the data base discussed in Section II below is an attempt to do so.

As experience with module fabrication improved it became possible to construct modules according to predictions based on design simulation. This allowed the gathering of actual outdoor data over extended periods to compare with model predictions and to refine the input to such models. One such study (Ref. 2) was a comparison of two types of 30x30 monolithic modules, one with half the cell width and hence twice the number of cells as the other. These so called "single and double string" (two parallel strings) modules are shown schematically in Fig. 1. A cross section of the monolithic design is shown in Fig. 2. The difference in outdoor performance of the two modules is shown in Fig. 3. The difference in performance was primarily attributed to differences in FF intensity dependence because of the contribution to series resistance of the transparent conductor. As shown below, on a peak performance basis, design B was 7% more efficient than A.

Ratio of:	FF	I_{sc}	Eff	Yearly Energy
Module B / Module A	1.13	0.95	1.07	1.05

Some of this advantage was lost on a comparison based on yearly energy delivery because of the lower average effective insolation that modules actually experience under real operating conditions. The choice of the best design had to be dictated in the final analysis by the application and by manufacturing economies.

A final area of particular interest to the TFS community is that of tandem modules. These are felt to be the means to achieving the 15-20% efficiency values needed for large scale implementation of PV (Ref. 3). These objectives are most likely to be met with Si top and Si/Ge alloy bottom devices. However, there are some potential near term advantages of Si/Si tandems over single cell devices (Ref. 4). A comparison of these module structures under actual outdoor conditions was recently undertaken (Ref. 5). The intent of the study was to gather data on actual performance to serve as input for modeling and simulation. A comparison of module output for a typical day is shown in Fig. 4. The modules with Si/Ge bottoms were observed to be less sensitive over the course of the day to changes in intensity and spectral content than their Si/Si counterparts. This is not unexpected and is primarily due to the greater spectral breadth of the Si/Ge alloys. As will be discussed below, the device thickness variations used in these structures have important stability implications. These will have to be included in future design efforts for tandem modules.

II. EFFECTS OF STABILITY

A. Stability Simulation

The details of stability related performance in TFS and the underlying mechanisms giving rise to this performance are still the subject of intensive study throughout the world. Just as the as-made performance varies from laboratory to laboratory, so also does the stability. The stability behavior of our devices is discussed in Ref. 6. In summary, we observe an initial loss of 10-15% which is a function of device thickness and details of preparation condition. The primary loss is in FF, with secondary losses sometimes observed in J_{sc} and V_{oc}. Output is then stable and does in fact improve during warm periods due to an annealing process. Most of the initial loss occurs during the first 20 hours of exposure.

In order to simulate these losses for module design purposes a simple approach was taken. In essence, it is found that stability losses can be nicely modeled by considering them simply as increases in series resistance. This was demonstrated by working with 4 cm^2 test structures and showing correlations between FF and the power curve slope at V_{oc}. This correlation for devices in the as-made state, B (before), and degraded state, A (after light exposure), is shown in Fig. 5. A change in slope of the unit corresponds to an increase in series resistance of ~0.67 ohm for these devices. This behavior is also a function of device thickness as shown in Fig. 6. The slopes of these lines is a measure of the bulk contribution to R_s in each of the states, while the zero thickness intercept is the interface contribution. It is seen then that the degraded state A derives from the B state through an increase in both bulk and interface components of R_s and will be modeled accordingly. Further details of this analysis will be provided elsewhere.

B. The Module Model

Details of the model used in this study are presented elsewhere (Ref. 2). For purposes of the discussion which follows, the aspect of interest is series resistance, R_s. There are two contributions to R_s, that due to the sheet rho of the electrodes and that due to contact resistance and to internal resistance of the photoactive material. The electrode resistance is dominated by typically high sheet rho's for transparent conductors and is described by standard distributed resistance formulas. The remaining components are lumped into the product of "R_c" and "contact length" (e.g. Fig. 7). What is shown as "R_{series}" in the data is the sum of these terms. Much of the analysis involves use of the R_c term to simulate degradation in terms of increases in series resistance as discussed above.

C. Module Performance

The starting point for this investigation is the power curve for an actual 30x30 cm module which is shown in Fig. 7. The module configuration is 25 series cells "single string" as shown in Figures 1 and 2. The data shown in the figure are actually the simulation that resulted in a fit to this actual measured curve for the module. The actual and simulated curves for the module exactly overlap at 7% efficiency and 0.54 FF. The manner in which the fit was achieved will now be discussed. In Fig. 8 the measured power curve is superimposed on a simulation of the "ideal" curve for the module. All of the data shown are for the ideal simulation. J_{sc}, J_o, n, T, area, module length, module width, cell width, cell length, and contact length are all variables whose known values as shown are input. R_{sq}, R_c and R_{shunt} are set at ideal values. The remaining parameters are calculated from this known set. As is seen, for $R_s = 0$ (total series resistance) and $R_{sh} \simeq$ (total shunt resistance), the module efficiency would be 8.75% with a 0.8 FF. It should be noted that the ideal FF of 0.8 agrees well with the extrapolated ideal from Fig. 6 for cells. The effect of including the known values of sheet resistance for the front (8 ohms/square) and rear (0.15 ohms/square) electrodes is shown in Fig. 9. These combine to result in a R_s = 2.8 ohms which reduces the FF to 0.74 and the efficiency to 8.2%.

Addition of the remaining series components will be accomplished by use of Fig. 6. First the contribution of the bulk photoconductor is calculated from the slope of the state B curve at a thickness of ~4500Å. For these 4 cm^2 test cells, a ~10% drop in FF is realized for each added ohm of R_s. Correcting this to the ~30 cm^2 cell areas in the module and to the fact that 25 such cells are in series results in the use of R_c = 0.0167 to effect an increase in R_s of ~1 ohm. This has only a minimal effect on FF, dropping it to 0.73 (Fig. 10). Again referring to Fig. 6 to get at the interface component of R_s, and again using the above corrections results in use of R_c = 0.071 and a resulting R_s = 6.8 ohms. This doubling of R_s due to the interface drops FF to 0.67 and efficiency to 7.3%. As can be seen in Fig. 11, the fit is close, but further adjustments are required.

All inputs to the model to this point are measured. Final fit however will be based upon observation rather than direct measurement. From the non-zero slope at I_{sc} of the measured power curve, it is apparent that some shunting should be included. The effect of adding R_{sh} = 1000 ohms-cm^2 (or ~33 ohms) is shown in Fig. 7. This simulated curve with only one adjusted parameter, R_{sh}, is an exact fit to the measured curve for the module.

The final step in the procedure is degradation of the module. This is accomplished by use of the state A data from Fig. 6. Combining both bulk and interface components results in R_c = 0.16 and R_s = 11.8 ohms. This increase in R_s of ~5 ohms drops FF to 0.56 and efficiency to 6.1% (Fig. 12), which corresponds directly to actual module behavior. It is to be noted that the degraded state was contributed to equally by bulk and interface losses. Solutions of either can bring module stability to the 95% vicinity.

A summary of the above procedures of first simulating and then degrading a module is given in Fig. 13. With the exception of a slight shunt loss, the entire process of loss is based upon accumulating series resistances. Opportunities for improving the as-made as well as stabilized performance of these modules lie with eliminating these resistances. Some implications of the present stability phenomena to module design are discussed in the following sections.

D. Design Issues

1. Transparent conductor (TC) sheet rho

Since TC sheet rho and degradation both contribute to R_s, the optimum sheet rho for a degraded module will not be the same as an as-made module. The effect of varying TC sheet rho for B and A states is shown in Fig. 14. In the high FF regime of low sheet rho, to first order there is little difference in the slopes of the B and A curves, and hence degradation is a non issue. Only at higher sheet rho values, where the degraded state starts asymptoting faster than the B state, is there some leverage. This is not a normal design regime for most applications however, and thus degradation does not play a significant role in module sheet rho choice. Broader, more leveraging issues such as transmission and cost trade-offs will still dominate.

2. Module cell density

For most current applications these modules have the constraint of generating voltages consistent with 12-volt battery charging or 12 volt devices. This and TC sheet rho largely drive cell size in 30x30 cm modules. The result is a series string of ~25 cells ~1 cm wide yielding V_{mp} of 13-15 volts.

As mentioned above and discussed in Ref. 2, paralleling allows other options on cell size. Additionally, other applications not tied to 12-volt systems, such as utility grid power, largely relax V_{oc} constraints. The effect on module design of relaxing this constraint is shown in Fig. 15. The trade-off that is occurring, as shown in Fig. 16, is that between FF and I_{sc}. FF increases with increasing cell density because the sheet rho contribution of the TC to R_s decreases as cell widths decrease. I_{sc} decreases in a straightforward way with decreasing cell width. Referring back to Fig. 15, it is seen that the 25-cell design is just below the efficiency peak which occurs at ~32 cells. Such a design would produce a V_{mp} of over 20 volts, which is inappropriate for 12-volt systems and thus useful only in non-constrained voltage applications.

The effect of degradation is only a small shift in the design point. This is demonstrated in Fig. 17, which is a plot of the percent of state B output maintained in state A. As can be seen, in terms of stability performance the current 25-cell design is nearly a full percentage point below the peak of maintained efficiency (~86.5 vs. ~87.5). In terms of stabilized output then, the optimum design point is ~35 cells (for non-constrained voltage applications).

CONCLUSIONS

The as made and degraded states of TFS based modules have been modelled in terms of series resistance losses. The origins of these losses lie in interface and bulk regions of the devices. When modules degrade under light exposure, increases occur in both the interface and bulk components of the loss based on series resistance. Actual module performance can thus be simulated by use of only one unknown parameter, shunt losses. Use of the simulation to optimize module design indicates that the current design of 25 cells per linear foot is near optimum. Degradation performance suggests a shift to ~35 cells to effect maximum output for applications not constrained to 12 volts. Earlier studies of energy based performance and tandem structures should be updated to include stability factors, not only the initial loss factor tested here, but also appropriate annealing factors.

ACKNOWLEDGEMENTS

Special thanks are extended to Kim Mitchell for use of the computer code and to Dennis Willett for cell thickness data.

REFERENCES

1. D.L. Morel, J.P. Rumburg, R.R. Gay and C.F. Gay, Proceedings of the Eighth Biennial Congress of the ISES, Perth, Australia, August 1983, p. 1517.

2. D.L. Morel, J.P. Rumburg, R.R. Cay, G.B. Turner and K.W. Mitchell, Proceedings of the 17th IEEE Photovoltaic Specialists Conference, Kissimee, Florida, May 1984.

3. G. Nakamura, K. Sato and Y. Yukimoto, Proceedings of the 16th IEEE Photovoltaic Specialists Conference, San Diego, California, September 1982, p. 1331.

4. Y. Hamakawa, H. Okamoto and Y. Nitta, App. Phys. Lett., 35(2), 187 (1979).

5. D.L. Morel, R.D. Wieting and K.W. Mitchell, Proceedings of the 1st International Photovoltaic Science and Engineering Conference, Kobe, Japan, November 1984, p.567.

6. H.S. Ullal, D.L. Morel, R.D. Wieting, D. Kanani, P.C. Taylor and C. Lee, Proceedings of the 17th IEEE Photovoltaic Specialists Conference, Kissimee, Florida, May 1984, p. 359.

Fig. 1
MODULE OPTIONS

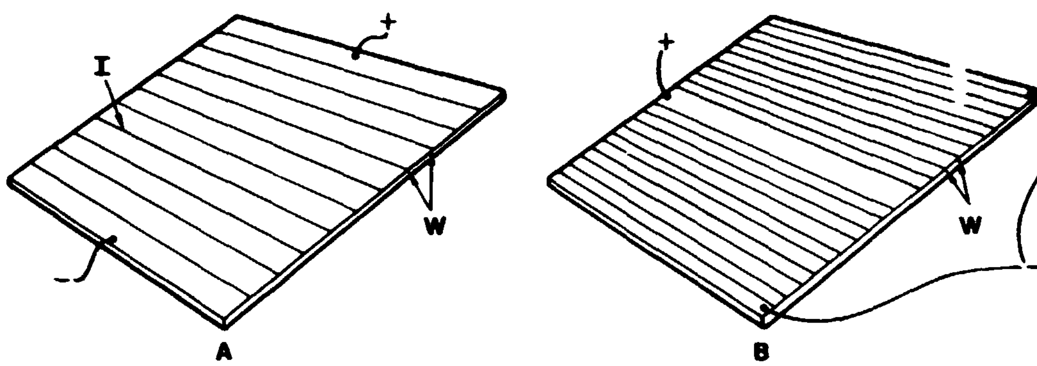

Single String
25 Series Connected Cells
1.0 cm Width
V_{mp} = 13 – 15 Volts

Double String
25 Series Connected Cells
0.5 cm Width
2 Parallel Strings
V_{mp} = 13 – 15 Volts

Fig. 2
MONOLITHIC MODULE CROSS SECTION

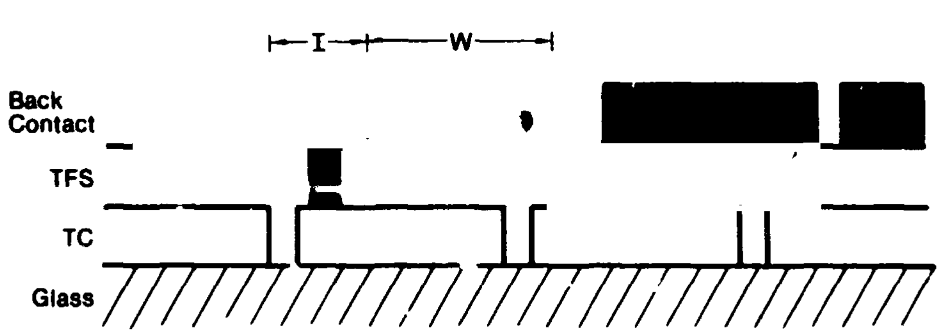

Fig. 13
MODULE FILL FACTOR LOSS MAP

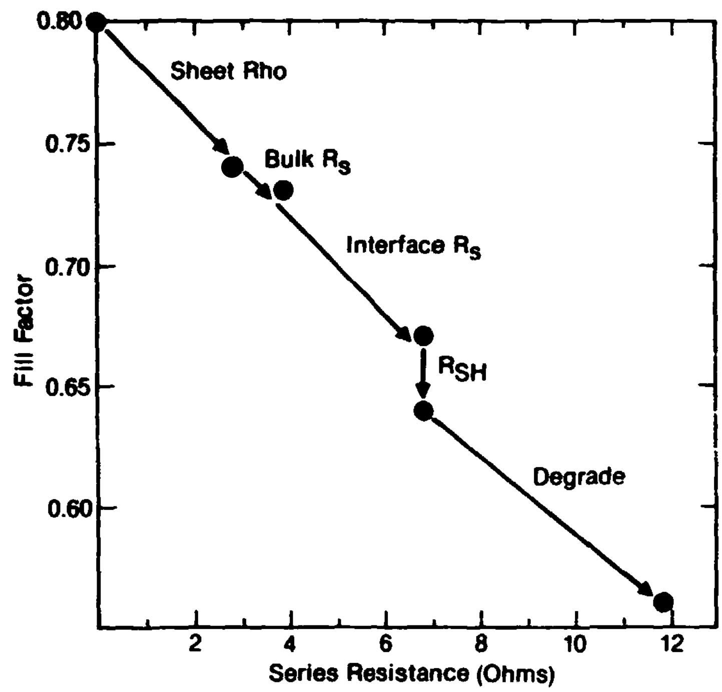

Fig. 14
MODULE FILL FACTOR VS. FR^NT ELECTRODE SHEET RHO

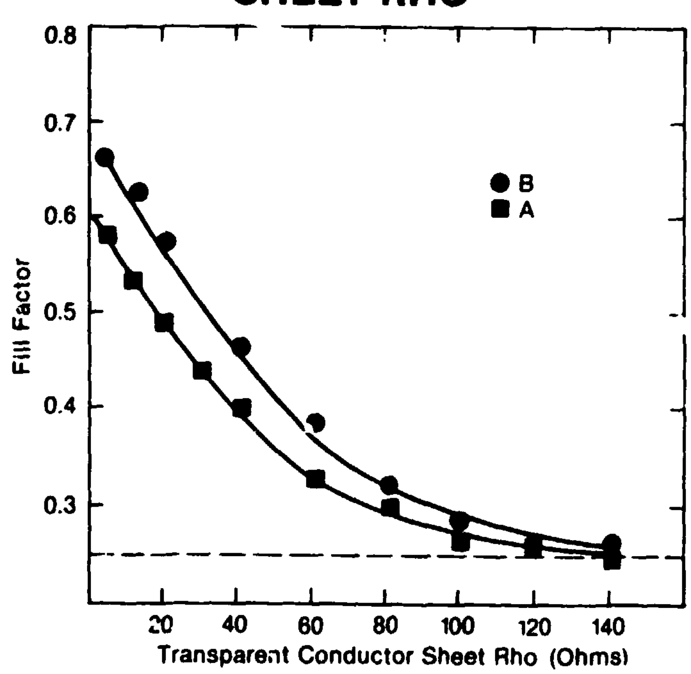

Fig. 3

ROOFTOP MODULE EFFICIENCY

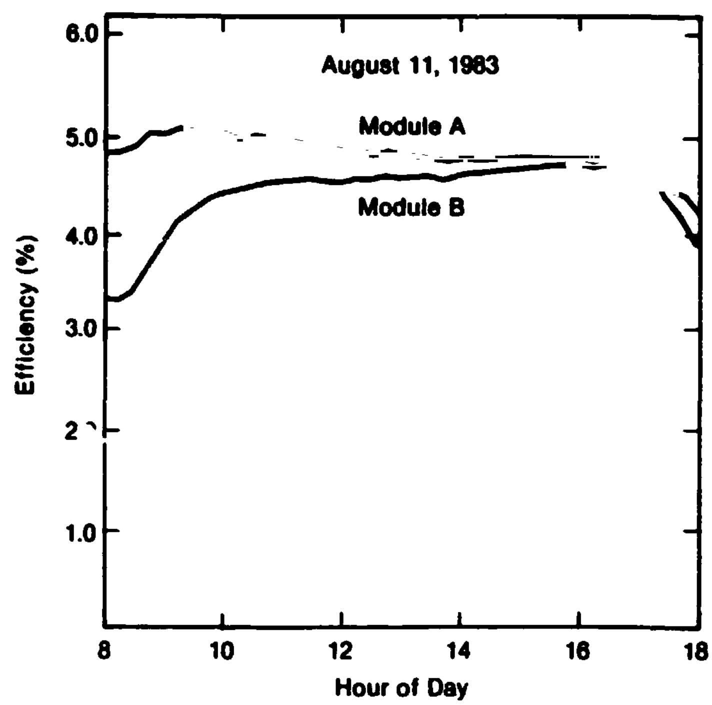

Fig. 4

Si/Si AND Si/Ge PERFORMANCE vs TIME

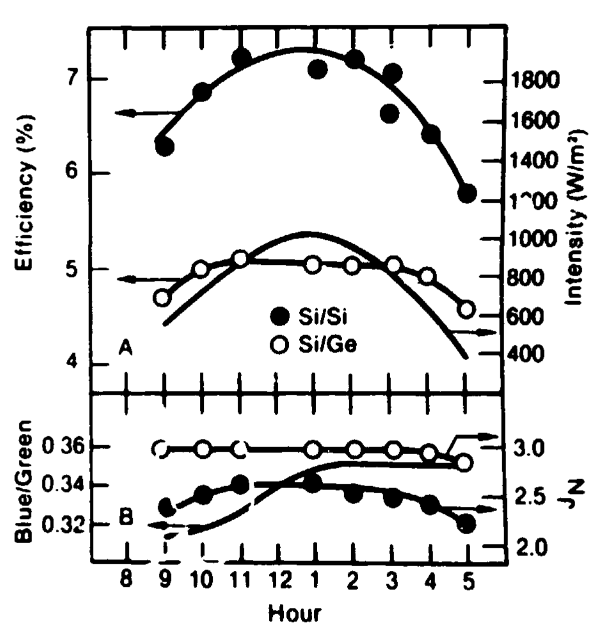

Fig. 5
SLOPE AT V_{OC} VS. FILL FACTOR FOR STANDARD CELL POPULATION IN B AND A STATES

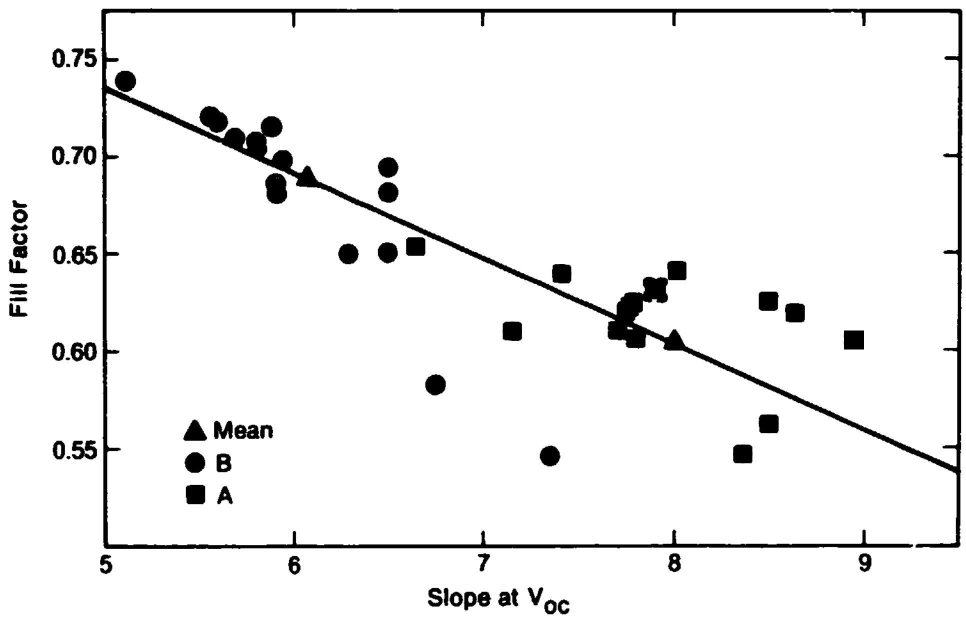

Fig. 6
FILL FACTOR VS. CELL THICKNESS FOR B AND A STATES

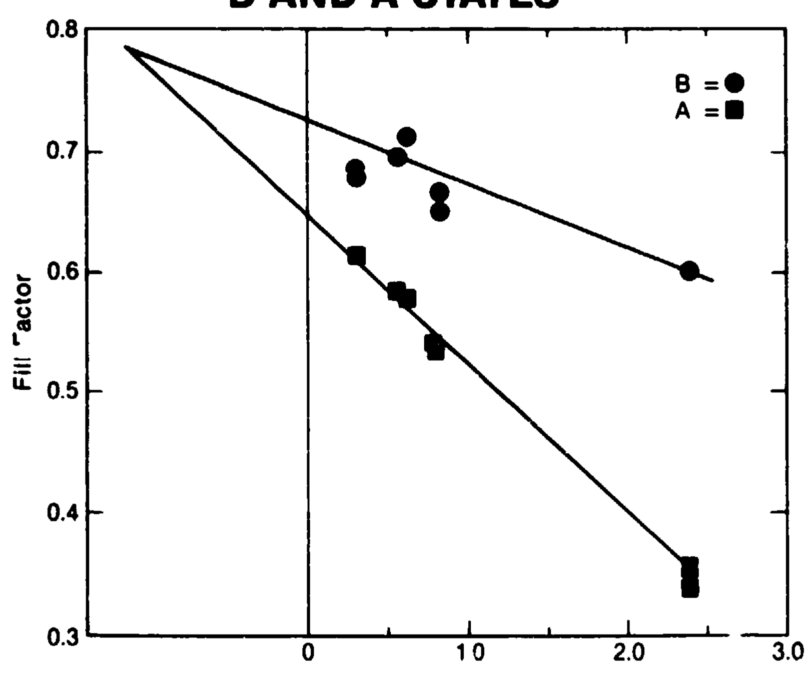

Fig. 7

MODULE I-V CURVE: R_{sh} INCLUDED

TFS 431 (1 String/25 Segments) Conc. = 1 sun
Shorted Segments = 0

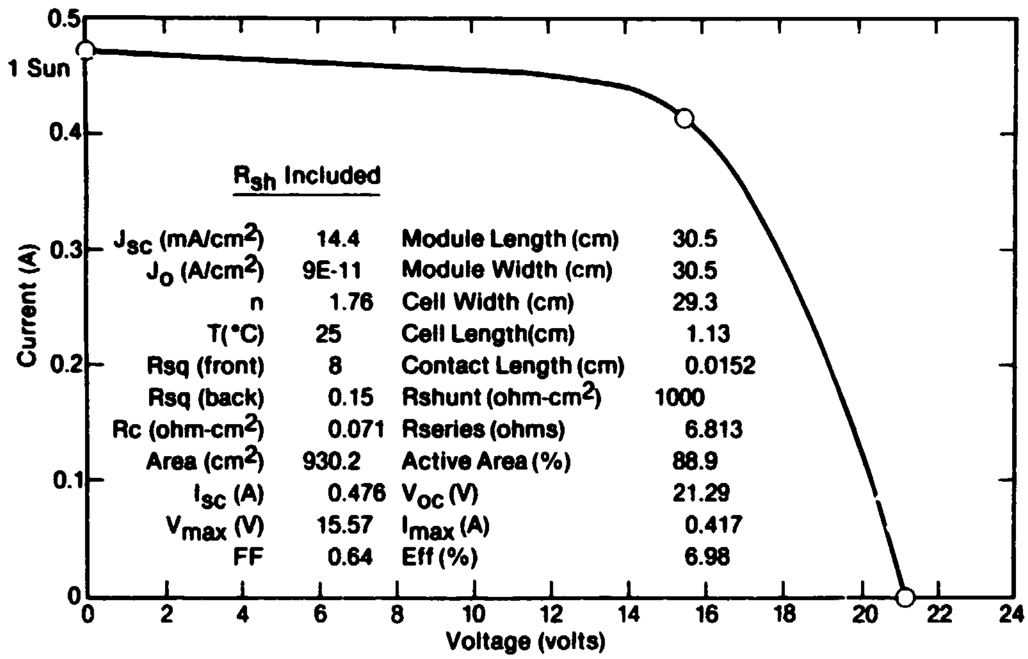

Fig. 8

MODULE I-V CURVE: IDEAL

TFS 431 (1 String/25 Segments) Conc. = 1 sun
Shorted Segments = 0

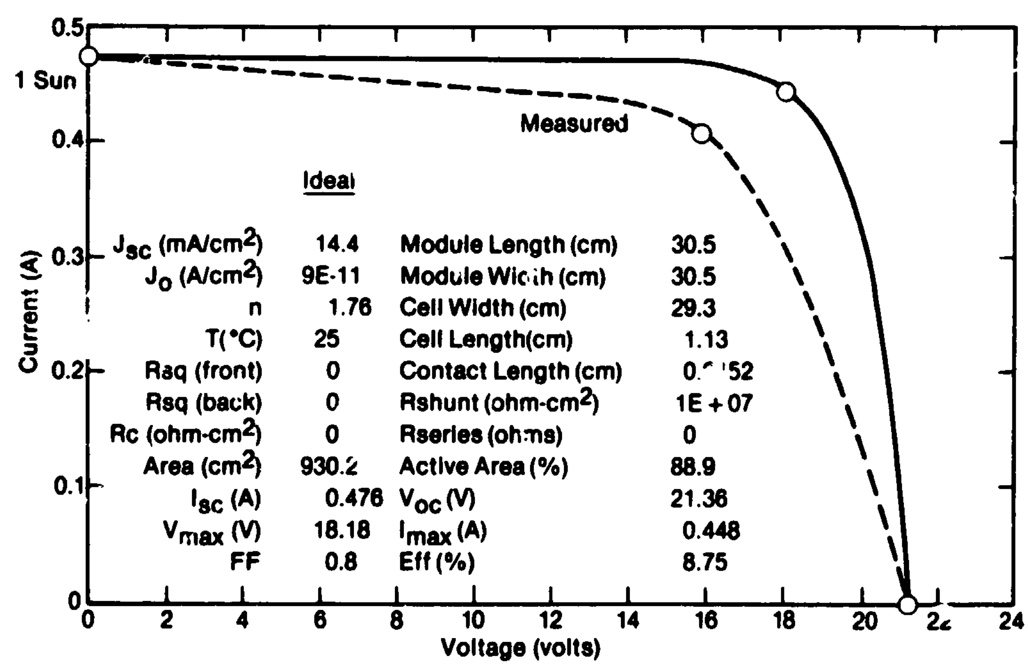

Fig. 9

MODULE I-V CURVE: SHEET RHO INCLUDED

TFS 431 (1 String/25 Segments) Conc. = 1 sun
Shorted Segments = 0

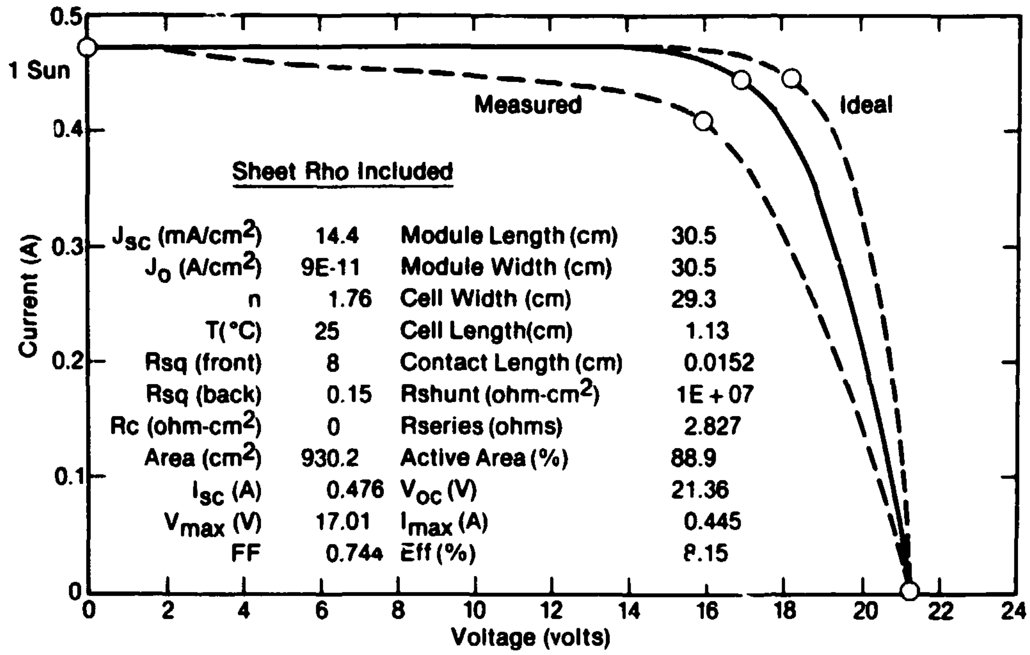

Fig. 10

MODULE I-V CURVE: BULK R_S INCLUDED

TFS 431 (1 String/25 Segments) Conc. = 1 sun
Shorted Segments = 0

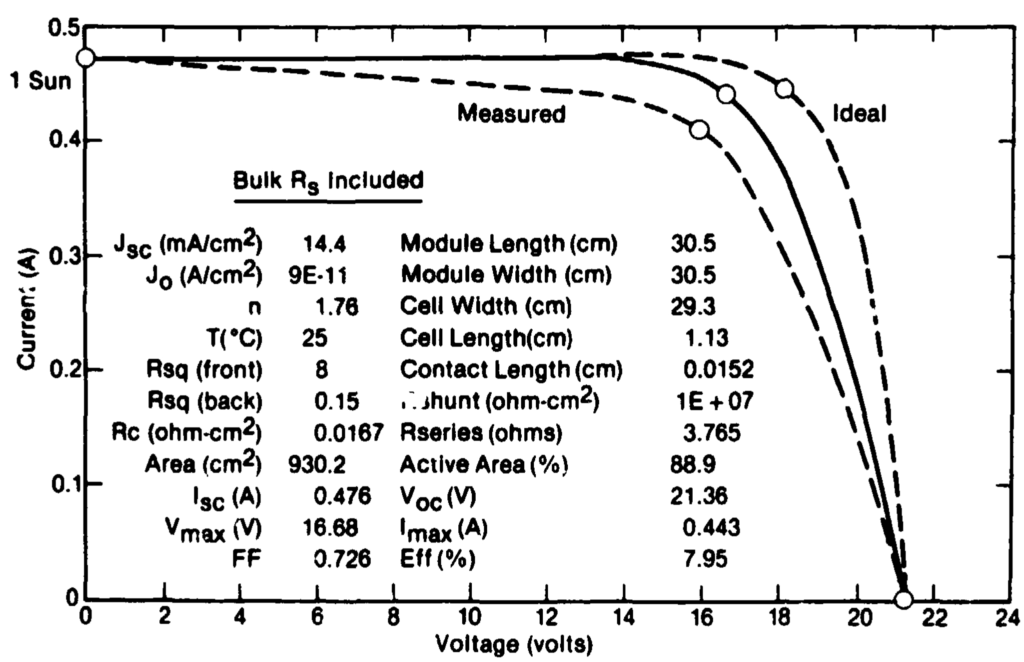

Fig. 11

MODULE I-V CURVE: INTERFACE R_S INCLUDED

TFS 431 (1 String/25 Segments) Conc. = 1 sun
Shorted Segments = 0

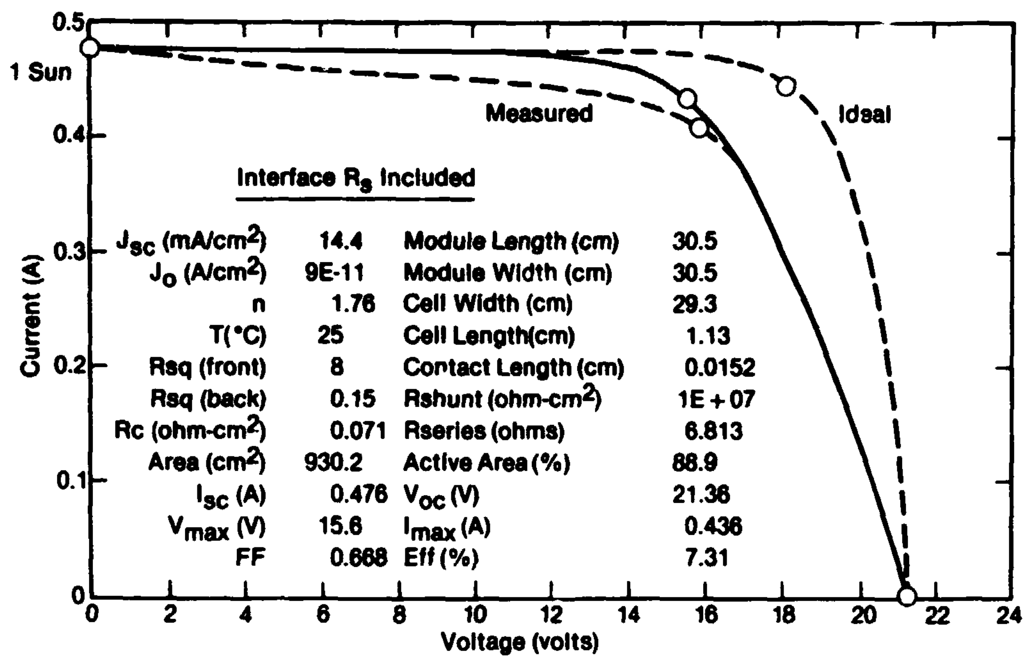

Fig. 12

MODULE I-V CURVE: DEGRADATION INCLUDED

TFS 431 (1 String/25 Segments) Conc. = 1 sun
Shorted Segments = 0

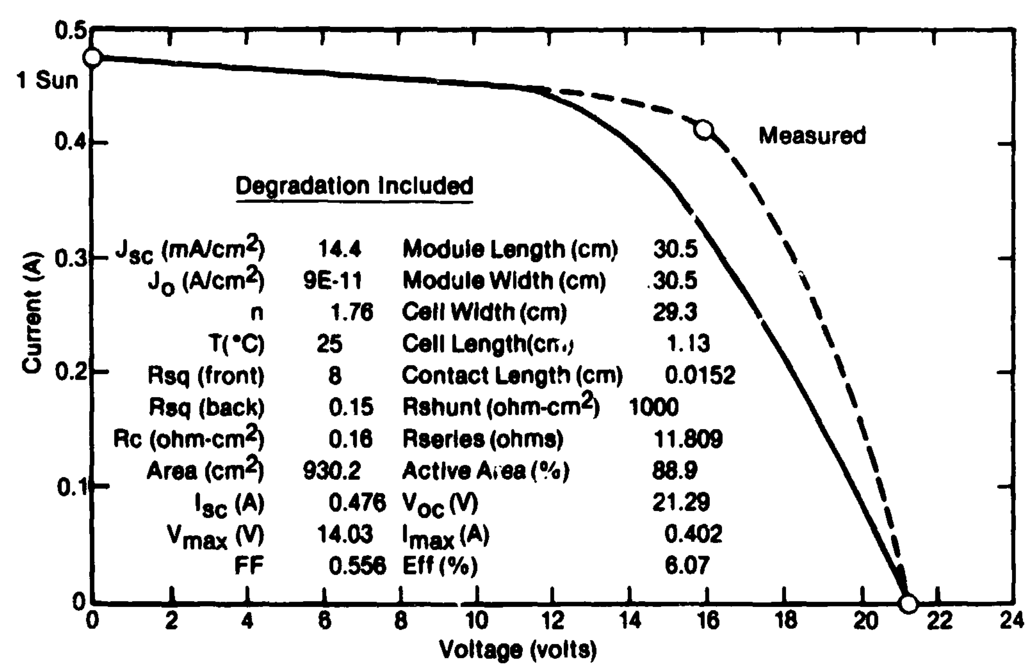

Fig. 15

MODULE EFFICIENCY VS. CELLS PER FOOT FOR B AND A STATES

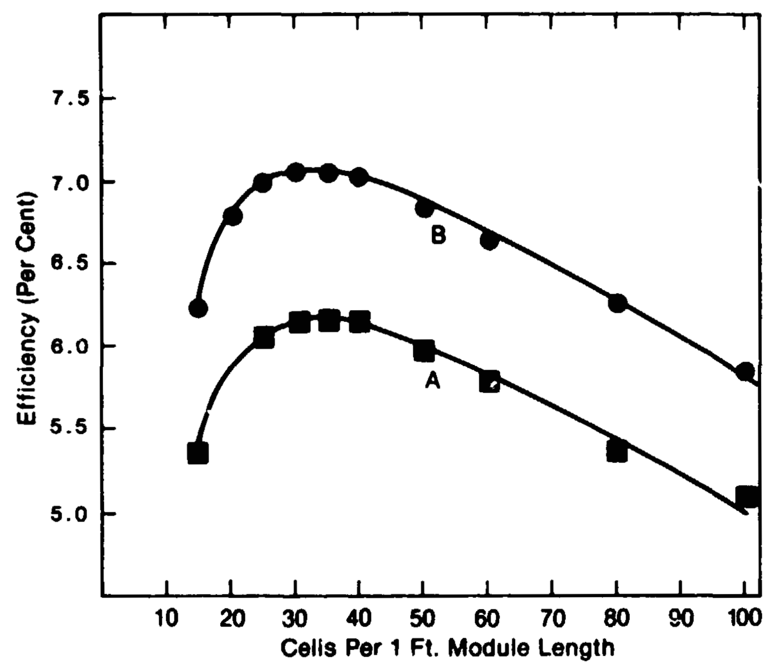

Fig. 16

FILL FACTOR AND SHORT CIRCUIT CURRENT VS. CELLS PER FOOT FOR B AND A STATES

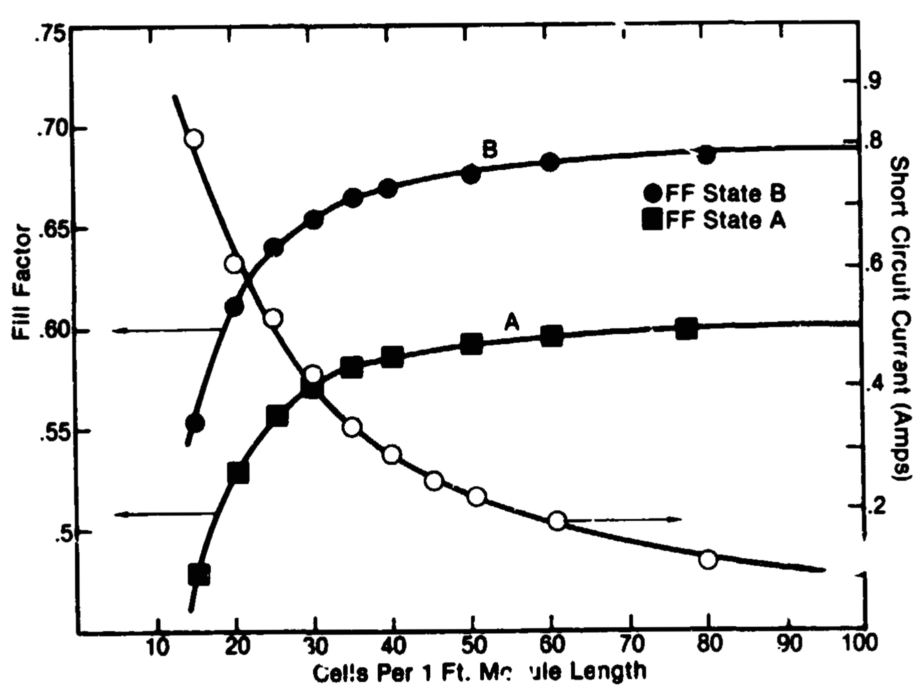

Fig. 17

PER CENT OF STATE B MAINTAINED BY A VS. CELLS PER FOOT

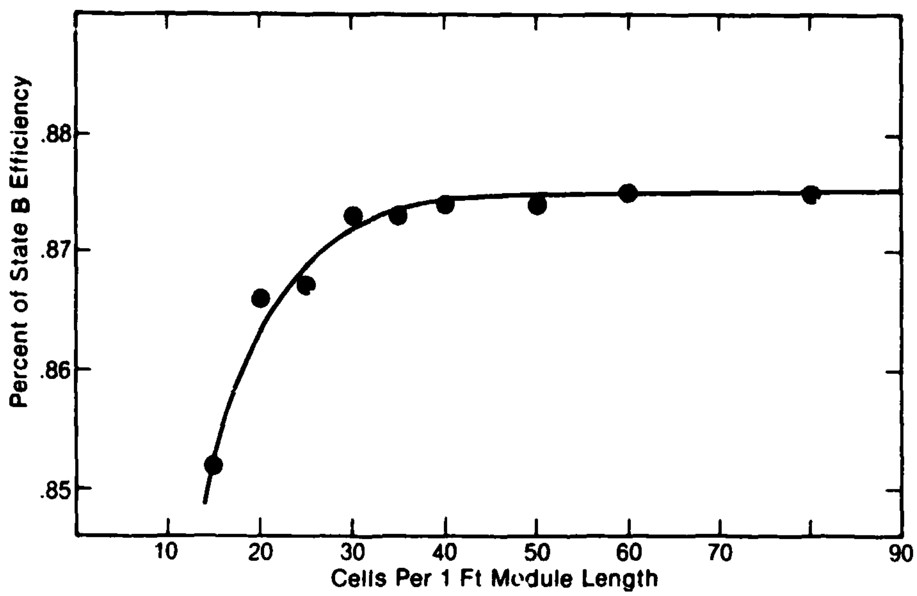

DISCUSSION

WRONSKI: You raised several very important questions. One is the difference between a tandem cell and a single cell; I think that should be taken into account. I have one question, though. It is very nice to parameterize the cell performance instead in terms of the R-shunt, R-series and so on. There is one difference I think between amorphous-silicon and crystalline-silicon cells, that the recombination per se rather than the series resistance can give characteristics that could be interpreted in terms of those parameters. I think that this should be pointed out, because it becomes very important when people start doing degradation studies and are looking for contact resistance and short resistance. But what I want to ask you is, have you got any feeling as to how we can tell the difference between the two mechanisms?

MOREL: Again I apologize, because what I'll say tomorrow addresses these very points you are making -- such as why this looks like series resistance. I have looked at it a little bit, the underlying physics, and it turns out that you picked one of the models in the literature that is a recombination model. I can come up with some things that come close to fitting what I have, although there are some wrinkles that are different in it. But I think the way to tell now is that there is an interface component and a bulk component. I think if we do some activation energy studies of annealing and so forth, we might be able to see the differences, and separate the two, and understand which is doing what.

LESK: I think it would be valuable from a modeling standpoint to show how your shunt resistance varies as a function of intensity. At night you would draw 12 amps reverse bias. That's got to drop very rapidly as a function of intensity in the dark. The shunt resistance basically has got to disappear. The energy is what looks like a function of intensity for modeling at less than one sun.

MOREL: I calculated what the current contribution of that was. Certainly, for the standard performance of the module out in the sunlight, light is not a big problem. But for the kind of issue you are raising, I don't know what the exact number would be if you calculated it out. We'd have to look at it more carefully to see how long it could stay in the dark before there is a problem. I don't know, offhand.

D'AIELLO: The interface component interests me. It looks very large in the module that you have. Do you have any thoughts on its origin, related to the physical effects?

MOREL: Truthfully, all of this was done in the last couple of weeks, and I have not had time to push it further than where it is right now, other than to try to relate the bulk part of it to some of the lifetime models. The interface part of it -- all I can do is speculate, and think that it has something to do with the p-transparent conductor interface, which seems to be a very sensitive thing. Also, one could point to the interface between the end and the back metal. There hav been some comments made already that some oxidation can take place there. I would not expect that to be reversible, however, and so we need to go back and look at some activation energies of reversibility and so forth to understand which parts of this are reversible and which are not. Then maybe we will understand.